



INSTITUTO DE INGENIERÍA ENERGÉTICA (Institute for Energy Engineering)

Research Publications

WARNING:

The following article appeared in Conference Proceedings or in a scientific Journal. The attached copy is for internal non-commercial research and education use, including for instruction at the authors institution and sharing with colleagues.

Other uses, including reproduction and distribution, or selling or licensing copies, or posting to personal, institutional or third party websites are prohibited. Please refer to the corresponding editor to get a copy

Study about the flashing process through a metering expansion valve

Mohammed Ait Bahajji, José M. Corberán *, Javier Urchueguía,
José González, Juventino Santiago

Instituto de Ingeniería Energética, Universidad Politécnica de Valencia, Camino de Vera 14, ES 46022 Valencia, Spain

Abstract

In this paper, the results from an experimental campaign about the flashing process occurring through a metering manual expansion valve, are presented and discussed. The results involved the measurement at different lifts of the flow-rate flowing through the valve for three different refrigerants R22, R290 (propane) and R410A. First the experimental rig is described and the employed instrumentation is commented upon and the corresponding uncertainties analyzed. The test matrix is then presented and discussed. Then the geometry of the valve is described and an analysis about its geometric throat area as a function of the valve lift is also presented. The results of mass flow rate for different upstream pressure and temperature, subcooling, and downstream pressure are presented and the effect of each of those operating condition on the obtained mass flow rate is discussed. Different flow models are applied in order to evaluate the effective flow area of the valve at every valve lift and a comparison study is performed in order to elucidate which is the model which better explains the obtained results. Finally the results obtained with the best estimate model are shown for the full collection of tested points and the three tested refrigerants.

© 2005 Elsevier Inc. All rights reserved.

1. Introduction

The industry of the Air Conditioning and Refrigeration are in a moment of transition caused by the environmental impact of the emissions of chlorine to the atmosphere. The chlorofluorocarbons (CFC) have a high destructive power of ozone stratospheric (ODP) due to their elevated chlorine content. By the Montreal protocol (1987), the production of these substances has been interrupted in most of the developed countries from 1996. The chlorine that contains hydrochlorofluorocarbons (HCFC) has a shorter time of life in the atmosphere and less ODP than the CFCs. In spite of that, in the last revision of the protocol of Montreal, the HCFCs was including also in the list of controlled substances, and a progressive reduction of its production was planned for its phase-out between 2020 and 2030.

In agreement with the described situation the necessity arises to found new refrigerants with adequate characteristics because a rapid phase-out of conventional refrigerants could paralyse the Air Conditioning and refrigeration industry. Before systems can be designed with alternative refrigerants, thermodynamic and thermophysical properties must first be characterised.

The expansion device is one of the fundamental elements in a refrigeration system. The role of an expansion device in a refrigeration cycle is first to maintain the pressure differential between the low pressure side (evaporator) and the high pressure side (condenser) for a compressor driven refrigerating process, second purpose is to regulate the refrigerant flow to match the heat flux in the heat exchangers. There are two types of expansion device: variable flow area devices and constant flow area devices.

The process of a refrigerant flow through an expansion valve is a flashing process, when the pressure of a liquid suddenly drops below its saturation pressure and the liquid passes from a subcooled to a superheated

* Corresponding author. Tel.: +34 963877323; fax: +34 963877329.
E-mail address: corberan@ter.upv.es (J.M. Corberán).

Nomenclature

A	area (m ²)	T_c	critical temperature (K)
D_0	orifice diameter (m)	T_r	reduced temperature (K)
h	valve lift (m)	T_{sat}	saturation temperature (K)
K	Boltzmann constant	v_f	specific volume of saturated liquid at initial temperature (m ³ /kg)
\dot{m}	mass flow rate (kg/s)	v_g	specific volume of saturated vapor at initial temperature (m ³ /kg)
Sub	subcooling (K)	α	angle (°)
P_{down}	downstream pressure (Pa)	Σ'	depressurization rate (Matm/s)
P_f	pressure at flashing inception (Pa)	σ	surface tension (N/m)
P_{sat}	saturation pressure at inlet temperature (Pa)	ρ	density (kg/m ³)
P_{up}	upstream pressure (Pa)		

state. An accurate knowledge of flashing phenomenon is essential in the determination (prediction) of critical flow rate.

Recent work on expansion devices has focused on constant flow area devices (capillary tubes and short tubes). Chen et al. [1] developed a correlation for metastable flow of refrigerant 12 through capillary tubes. The short tube has studied with R12 and R22 [2], with R134A [3,4] and with R407C [5].

In this study, a manual expansion valve with possibility of changing the position of the needle, operated with a micrometer mechanism, was characterised for HCFC-22 and two alternative refrigerants R290 (propane) and R410A (HFC-32/HFC-125). Experimental results of the present investigation demonstrated the effect of the upstream pressure, upstream subcooling, downstream pressure and valve lift on the mass flow rate in a wide range operation of heat pump and refrigeration system. In addition, different flow models are used in order to evaluate the effective flow area of the valve at every valve lift and all results of each model are shown.

2. Experimental apparatus and procedure

Fig. 1 shows a schematic diagram of the refrigeration components characterization test rig used for the measurement of basic characteristics of manual expansion valve. In order to characterize the manual expansion valve, labelled SS-4BMRG from Swagelok, with different refrigerants two scroll compressors has been used, one labelled SM115S4, from Danfoss Maneurop, for R22 and R290 and the other one labelled ZP54K3E-TFD, from Copeland, for R410A.

Several PID control loops (expansion valve inlet and outlet pressure, subcooling and superheat controls) were incorporated to allow a precise adjustment of the refrigerant conditions at expansion valve inlet (condensing pressure and subcooling) and outlet (evaporating pressure). The rig was thus fully automated, making it pos-

sible to reach any allowable test conditions without manual adjustments.

Safety was a major concern during the conception of the test facility, since the propane was going to be employed. Specific procedures and standards regarding the managing and use of flammable gases were taken into account. These specific measures included the use of intrinsically safe electric material, special propane sensors, the use of emergency switches and alarms and appropriate air renewal procedures to ensure non-critical concentrations in case of leakage.

The mass flow rate was measured by coriolis-type (Fisher-Rosemount Micro-Motion CMF025M) and was compared with the secondary refrigerant calorimeter model, because it is the determining parameter to be analysed. The instrument accuracies of pressure transmitter (Fisher-Rosemount 3051) and temperature transmitter (RTD-PT 100 Ω), given by the calibration certificate of the manufactures, are $\pm 0.02\%$ and ± 0.1 K, respectively.

The test matrix used for the characterization of the manual expansion valve was chosen taking account typical operating conditions of Heat Pumps and Air Conditioners (see Table 1), with 280 data points in total. All measurements were carried out at steady-state conditions with the following fluctuations: inlet temperatures (subcooling) ± 0.1 K; mass flow rate $\pm 0.5 \times 10^{-3}$ kg/s; inlet pressure $\pm 0.02 \times 10^5$ Pa and outlet pressure $\pm 0.01 \times 10^5$ Pa (see Fig. 2).

3. Valve geometry

In order to quantify relevant parameters, the valve was disassembled and its geometrical characteristics were accurately measured in a metrology laboratory. Fig. 3 shows the geometry of the throttling section of the valve. The main geometric magnitudes turned out to be:

$$D_0 = 4.25 \times 10^{-3} \pm 0.04 \times 10^{-3} \text{ m}$$

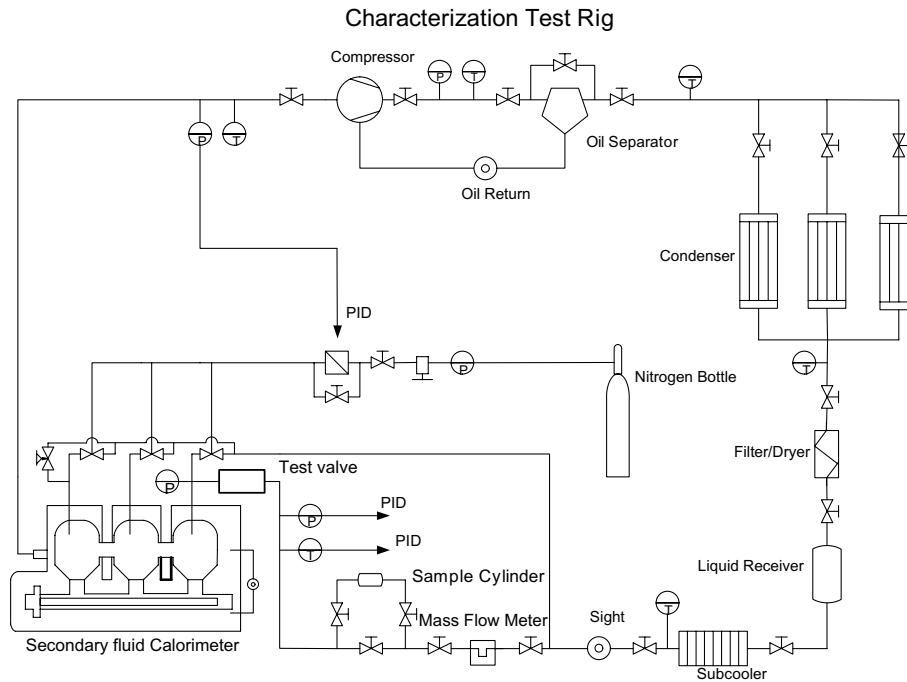


Fig. 1. Schematic of the experimental setup for the characterization of the manual expansion valve.

Table 1
Test matrix of manual expansion valve

Refrigerant	$T_{\text{sat}} (P_{\text{up}})$ (K)	$P_{\text{up}} (10^5 \text{ Pa})$	Sub (K)	$h (10^{-3} \text{ m})$
R22	313.15	15.34	5.6	0-4.064
			9.7	0-4.064
			13.9	0-4.064
	318.15	17.23	5.6	0-4.064
			9.7	0-4.064
			13.9	0-3.048
	323.15	19.43	5.6	0-4.064
			9.7	0-4.064
			13.9	0-2.032
R290	313.15	13.69	5.6	0-2.54
			9.7	0-2.54
			13.9	0-2.54
	318.15	15.34	5.6	0-2.54
			9.7	0-2.54
			13.9	0-2.54
	323.15	17.13	5.6	0-2.54
			9.7	0-2.54
			13.9	0-2.032
R410A	313.15	24.17	5.6	0-1.524
			9.7	0-1.524
			13.9	0-0.6604
	318.15	27.24	5.6	0-1.016
			9.7	0-0.762
			13.9	0-0.6604
	323.15	30.61	5.6	0-0.762
			9.7	0-0.762
			13.9	0-0.6604

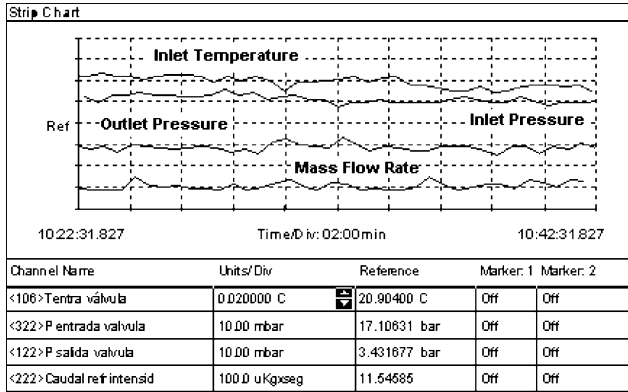


Fig. 2. Sample of measurement fluctuations at steady-state.

$$\alpha = 9.7 \pm 0.2^\circ$$

The measured orifice diameter was in perfect agreement with the information supplied by the manufacturer in the catalogue.

The geometric throat area can be estimated by the following expression:

$$A = \pi h \left[D_0 \sin(\alpha) - \frac{h \sin^2(2\alpha)}{4 \cos(\alpha)} \right] \quad (1)$$

4. Results

4.1. Effect of downstream pressure on mass flow rate

Fig. 4 shows the effects of downstream pressure on the mass flow rate with three different refrigerants (R22, R290 and R410A) and different lift conditions, where the downstream pressure, P_{down} , was always

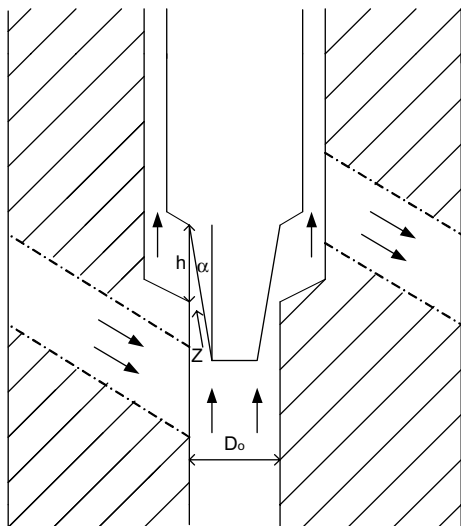


Fig. 3. Geometry of the expansion valve.

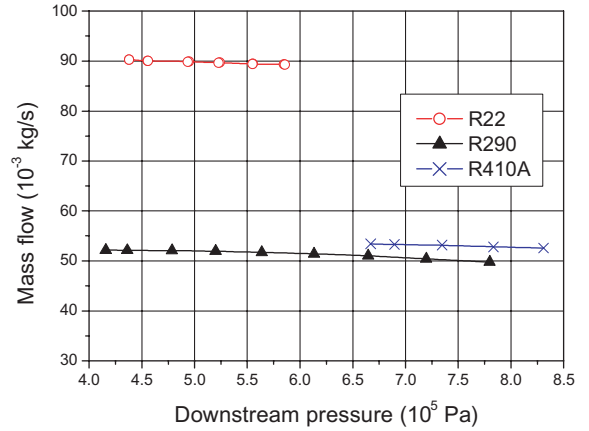


Fig. 4. flow dependency on downstream pressure for following conditions: R22: $P_{up} = 15.34 \times 10^5$ Pa, $Sub = 13.9$ K, $h = 1.016 \times 10^{-3}$ m. R290: $P_{up} = 13.69 \times 10^5$ Pa, $Sub = 13.2$ K, $h = 1.016 \times 10^{-3}$ m. R410A: $P_{up} = 20.02 \times 10^5$ Pa, $Sub = 7.7$ K, $h = 0.254 \times 10^{-3}$ m.

much lower than liquid saturation pressure, P_{sat} , corresponding to the upstream temperature. As can be observed, the mass flow rate of refrigerant was almost insensitive to downstream pressure, just a very slight decrease 2–5% of the mass flow rate was found when the downstream pressure was increased.

In choked flow conditions, the mass flow rate remains constant with further reduction in downstream pressure. Therefore, the flow of refrigerant through expansion valve does satisfy approximate ideal choked flow conditions. In review of the literature, this phenomenon was observed in short tube orifices [2,3,5] and capillary tubes [6]. But of course, it is common to any expansion device in refrigeration systems.

4.2. Effect of upstream pressure on mass flow rate

Fig. 5 shows the variation in mass flow rate with upstream pressure, where the abscis axis represent the saturation temperature (condensation) corresponding to upstream pressure for each refrigerant. As can be observed, the mass flow rate is proportional to upstream pressure by keeping the subcooling, the downstream and valve lift constants.

Aaron and Domanski [2] noted two separate factors to explain the effects of upstream pressure on mass flow rate. For a constant subcooling, as the upstream pressure increases, the upstream liquid density decreases due to fluid temperature increasing. This first effect tends to decrease the mass flow rate. But the allowable subcooled pressure drop, the difference between the upstream pressure and saturation pressure increases. This second effect tends to increase the mass flow rate because once the fluid flashes, the fluid becomes approximately choked.

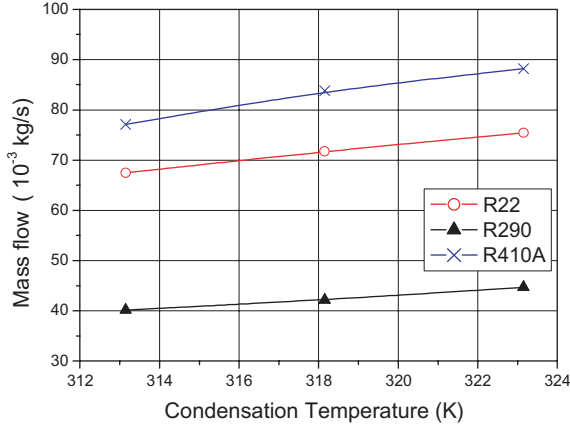


Fig. 5. Flow dependency on upstream pressure (condensation temperature) with constants subcooling (5.6 K) and valve lift (0.6604×10^{-3} m).

Therefore, the effect of allowable subcooled pressure is more dominant than the effect of density on mass flow rate. These trends are also observed in published literature with capillary tubes and short tube orifices.

4.3. Effect of upstream subcooling on mass flow rate

To see the effects of the upstream subcooling on mass flow rate through the expansion valve, a series of tests were performed, where the upstream pressure was set to three different values and the upstream subcooling has been varied from 5.6 K to 13.9 K at different valve lifts (see Table 1). Fig. 6 shows the mass flow rate through the expansion valve as a function of the upstream subcooling for 0.6604×10^{-3} m valve lift. As can be observed, the mass flow rate clearly increases with increasing the upstream subcooling.

The effects of subcooling on the mass flow rate can be described by two factors. For a constant upstream pres-

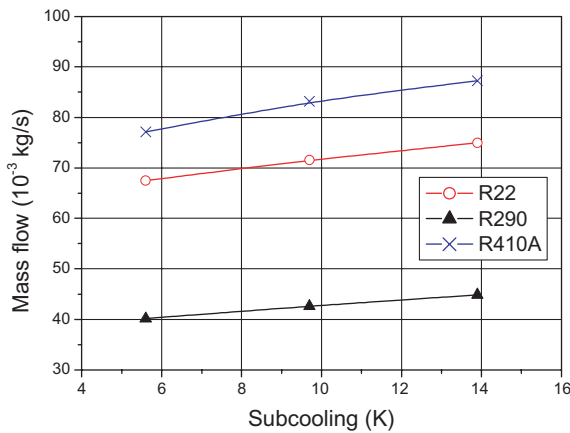


Fig. 6. Flow dependency on upstream subcooling with constants condensation temperature (313.15 K) and valve lift (0.6604×10^{-3} m).

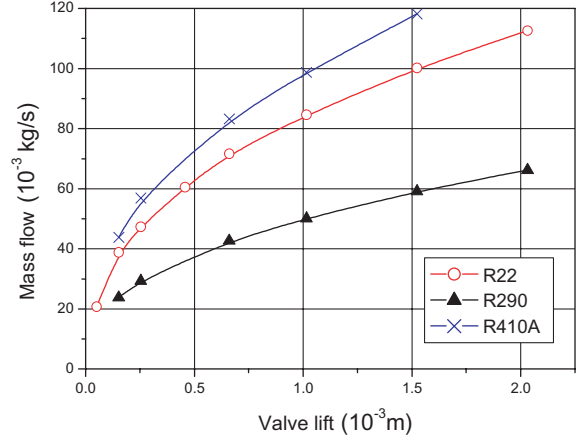


Fig. 7. Flow dependency on valve lift at constant condensation temperature (313.15 K) and subcooling (9.7 K).

sure, as the upstream subcooling increases, the upstream density increases due to fluid temperature decrease. Thus, the mass flow rate tends to raise. Also, the second factor caused by the increase of the subcooling tends to increase the mass flow rate due to the allowable subcooled pressure drop.

4.4. Effect of valve lift on mass flow rate

Fig. 7 shows the influence of valve lift on mass flow rate for the three tested refrigerants (R22; R290 and R410A) with a subcooling of 9.7 K and the same saturation temperature, 313.15 K, corresponding to upstream pressure for each refrigerant R22: $P_{up} = 15.34 \times 10^5$ Pa; R290: $P_{up} = 13.69 \times 10^5$ Pa; R410A: $P_{up} = 24.17 \times 10^5$ Pa. As can be observed, the mass flow rate increases due to the increase of the flow area at the valve throat when the valve lift is increased.

The propane mass flow rate is lower than R22 and R410A due to its lower density. However, it is interesting to observe that R410A give higher mass flow rate than R22, in spite of its lower density than R22, due to its higher allowable subcooled pressure ($P_{up} - P_{sat}$)_{R410A} > ($P_{up} - P_{sat}$)_{R22}. Therefore, this might indicate that the allowable pressure drop has a greater influence on mass flow rate than the upstream liquid density.

5. Effective flow area

Fig. 8 presents the geometric throat area expressed by Eq. (1) as a function of valve lift (solid line).

In order to evaluate the effective flow area, different flow models are applied under different hypothesis. Reviewing the literature, Alamgir [7]; Abuaf [8]; Shin [9]; Blinkov [10], for flashing of initially subcooled liquid, found that void development upstream of the

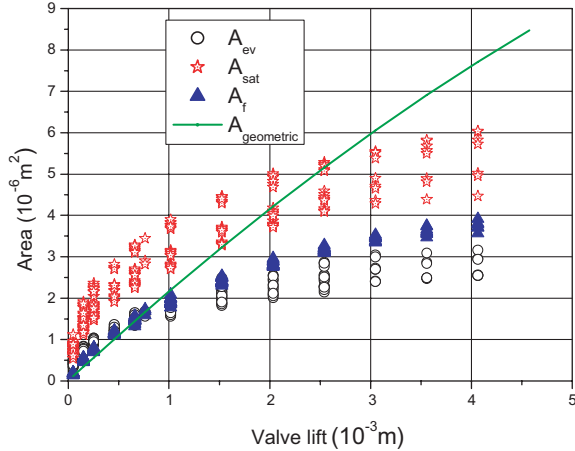


Fig. 8. Different effective flow area models.

throat was negligible: within 1–2% void fraction at the throat. Thus the flashing flow with subcooled inlet condition remains almost single-phase flow upstream of the throat. Then, the flashing mass flow rate can be calculated by the conventional Bernoulli equation. Therefore, the effective flow area can be estimated from:

$$A_i = \frac{\dot{m}}{\sqrt{2\rho(P_{up} - P_i)}} \quad (2)$$

where P_i is the pressure at the throat (or minimum cross-section). The problem arises in how to know or measure that pressure. Several options are found in the technical literature.

When the pressure at the vena contracta was near to liquid saturation pressure, P_{sat} , corresponding to inlet temperature, P_i was typically replaced by P_{sat} . As can be observed in Fig. 8, the effective flow area A_{sat} , given by this model, was clearly higher than the geometric throat area in a wide range of valve lift. In addition, the dispersion of results becomes very higher, clearly showing that this hypothesis is far from reality in refrigeration expansion devices.

The manufacturers of expansion valves provide catalogues where P_i was replaced by, P_{ev} , pressure downstream of valve (evaporation pressure) to calculate the mass flow rate by means of Eq. (2). In this case, the dispersion of effective flow area is significant as can be seen in Fig. 8 (see curve A_{ev}).

Most investigators, among them Alamgir [7]; Chen [1]; Xu [11]; Dekang [4], applied the basic nucleation theory to predict the pressure undershoot, $P_{sat} - P_f$, the pressure difference between the thermodynamic saturated pressure and the minimum pressure in a depressurization process. Alamgir [7] developed a semiempirical correlation (Eq. (3)) for predicting of the pressure undershoot based on static decompression effects. Subsequently, Abuaf [8] combined that effect with the equa-

tion of depressurization rate, Σ' , given by Eq. (4) to predict critical flashing flow with the following formulas:

$$P_{sat} - P_f = 0.253 \frac{\sigma^{\frac{3}{2}} T_R^{13.73} \sqrt{1 + 14\Sigma'^{0.8}}}{\sqrt{KT_c} \left[1 - \frac{v_f}{v_g}\right]} \quad (3)$$

$$\Sigma' = \frac{\dot{m}^3}{\rho^2 A_f^4} \frac{dA}{dz} \quad (4)$$

where $\frac{dA}{dz}$ can be calculated from Eq. (1), so that:

$$\frac{dA}{dz} = \frac{dA}{dh} \frac{dh}{dz} = \left[D_0 \sin(\alpha) - \frac{h \sin^2(2\alpha)}{2 \cos(\alpha)} \right] \frac{\pi}{\cos(\alpha)} \quad (5)$$

The above system of equations (closed with Eq. (2)) is implicit in the effective flow area (A_f). Eq. (4) also includes a term involving the variation of the flow area with the longitudinal coordinate, $\frac{dA}{dz}$. We have preferred to evaluate this term from the derivative of the geometric throat area (Eq. (5)) in order to reduce the implicitness of the system of equations.

The system of equations can be solved for every measured point providing the value of the effective flow area for each point. These results are also shown in Fig. 8 and, as can be observed, the obtained curve is much lower, leading to just an almost single flow area line for all the measured points. Therefore, it can be concluded that this model is the one which best represents the flashing flow at the valve.

However, the obtained values for low lifts are greater than the geometric throat area. The authors are studying the geometric throat area of the valve with more detail, mainly the seat of the poppet at the throat, trying to find an explanation to this paradox.

6. Conclusions

This study presents new experimental data for the critical flow through a metering manual expansion valve, with HCFC-22 as reference refrigerant and two different alternative refrigerant: R290 (propane), as pure refrigerant, and R410A, as azeotropic mixture (HFC-32/HFC-125). The mass flow rate was characterized for a wide range of conditions covering Heat Pump and Air Conditioning operation.

Mass flow rate was found to be almost insensitive to downstream pressure, clearly indicating choked flow conditions. Also, experimental results show that by increasing the upstream pressure or the upstream subcooling the mass flow rate is increased.

An analysis employing the Bernoulli incompressible flow formula has allowed the estimation of the effective flow area under different hypothesis for the throat pressure. This analysis proves that the best model to

be employed is the one based on the classic nucleation theory, and allows the accurate calculation of the circulating mass flow rate.

References

- [1] Z.H. Chen, R.Y. Li, S. Lin, Z.Y. Chen, A correlation for metastable flow of refrigerant 12 through capillary tubes, *ASHRAE Trans.* 96 (1) (1990) 550–554.
- [2] A.A. Aaron, P.A. Domanski, Experimentation, analysis and correlation of refrigerant-22 flow through short tube restrictors, *ASHRAE Trans.* 96 (1) (1990) 729–742.
- [3] Y. Kim, Two-phase flow of HCFC-22 and HFC-134A through short-tube orifices, Ph.D. thesis, Texas A&M University, College Station, 1993.
- [4] Dekang Chen, Sui Lin, Under pressure of vaporization of refrigerant R134A through a diabatic capillary tube, *Int. J. Refrig.* 24 (2001) 261–271.
- [5] W.V. Payne, D.L. O'Neal, Mass flow characteristics of R407C through short-tube orifices, *ASHRAE Trans.* 104(1) (1998) 197–209.
- [6] M.B. Pate, D.R. Tree, An analysis of choked flow condition in a capillary tube-suction line heat exchanger, *ASHRAE Trans.* 93 (1) (1987) 368–380.
- [7] Alamgir, J.H. Lienhard, Correlation of pressure undershoot during hot-water depressurization, *J. Heat Transfer, Trans. ASME* 103 (1981) 52–55.
- [8] N. Abuaf, O.C. Jones, B.J.C. Wu, Critical flashing flows in nozzles with subcooled inlet conditions, *J. Heat Transfer, Trans. ASME* 105 (1983) 379–383.
- [9] T.S. Shin, O.C. Jones, Nucleation and flashing in nozzles-1 a distributed nucleation model, *Int. J. Multiphase Flow* 19 (6) (1993) 943–964.
- [10] V.N. Blinkov, O.C. Jones, B.I. Nigmatulin, Nucleation and flashing in nozzles-2 comparison with experiments using a five equation model for vapor void development, *Int. J. Multiphase Flow* 19 (6) (1993) 965–986.
- [11] J.L. Xu, T.K. Chen, X.J. Chen, Critical flow in convergent-divergent nozzles with cavity nucleation model, *Exp. Thermal Fluid Sci.* 14 (2) (1997) 166–173.